The Role of Hydrogen Partial Pressure in the Gas-Phase Hydrogenation of Aromatics over Supported Nickel

Mark A. Keane*,† and Patricia M. Patterson‡

Department of Chemical Engineering and Department of Fuel and Energy, The University of Leeds, Leeds LS2 9JT, U.K.

The effect of varying the hydrogen partial pressure (from 0.19 to 0.96 atm) on turnover frequencies (TOFs) in the gas-phase hydrogenation of benzene, toluene, and *o*-, *m*-, and *p*-xylene over a Ni/SiO_2 catalyst has been studied. Each system is characterized by well-defined reversible temperature related activity maxima (T_{max}) where T_{max} was shifted in the conversion of benzene and toluene to lower values as the hydrogen partial pressure was reduced but remained unaffected in reactions involving the isomers of xylene. The range of TOFs reported for each aromatic system and the occurrence of T_{max} are explained on the basis of interplay between the supply and reactivity of active surface species. The observed relationships between reaction temperature and TOF are represented by means of a common extended power rate model. The nature of true and apparent reaction kinetics is discussed, and a compensation effect is established wherein the only reaction variable is the hydrogen partial pressure. The experimentally determined activation energies do not represent the true catalytically relevant energetics because of the existence of preequilibria to the rate-determining step. The measured Arrhenius parameters are shown to be composite terms and are pressure dependent. Catalytically significant heats of adsorption have been extracted from the reaction data, and the TOFs have been found to be inversely proportional to the magnitude of the heat of adsorption of hydrogen.

Introduction

The heterogeneous hydrogenation of aromatic compounds not only is a useful model reaction to gauge the activity of metal catalysts but also is of commercial importance in the upgrading of coal liquids[1] and of environmental significance in reducing undesired emissions in exhaust gases.[2] The hydrogenation of benzene over a range of transition-metal catalysts is well-documented,[2,3] and the activity of unsupported nickel[4−6] and nickel supported on amorphous[4,7−17] and zeolite[17−20] carriers is now established. Briefly, the reported benzene/hydrogen/nickel reaction systems have been variously characterized by the following features: (a) rate maxima at 423,[15] 453,[6,8,14] and 473 K;[16,19] (b) rate inhibition by the product (cyclohexane);[5,6] (c) rapid desorption of cyclohexane with no rate inhibition;[8,14,16,20] (d) competitive adsorption of benzene and hydrogen;[7] (e) noncompetitive adsorption of benzene and hydrogen;[14,16,17,20,21] (f) a temperature dependence of the reaction order with respect to the benzene and hydrogen partial pressures that varied from 0 to 0.5[4−9,11,12,14,16,17,22] and from 0.5 to 3,[4−9,11,12,15−17,19] respectively; (g) apparent activation energies in the range of 25−94 kJ mol^{-1}.[4−11,16,19] The source of such discordant reports can be attributed, at least in part, to incomplete or insufficient kinetic studies. Indeed, Bond et al.[23] have eloquently expressed the limitations inherent in many kinetic studies of heterogeneous catalysis. Given the complexity and multivariable nature of the systems involved, the discrepancies in the kinetic observations catalogued above may also be ascribed to variations in process conditions. Moreover, the role of catalyst preparation, the nature of the metal precursor and support (surface area, porosity, chemical purity, and/or functionality), and the ultimate dispersion/dimensions of the active metal phase can certainly have a bearing on the catalytic data. It is, however, difficult to gauge the relative importance of each catalyst variable on performance where benzene hydrogenation, for instance, has been characterized as both structure-sensitive[4,15,17] and insensitive.[7,9,11]

Benzene has thusfar been the overwhelming model aromatic reactant, and a limited number of reports have emerged dealing with toluene hydrogenation over nickel catalysts[24] where the focus was placed on the electronic effects induced by the methyl substituent on the degree of ring reduction. The hydrogenation of xylene(s) has received even less attention, and the available data are generally in the form of rate ratios relative to a benzene feed.[3] Recently, Rahaman and Vannice[25] working with palladium-based catalysts and Salmi et al.[26−30] with nickel-based catalysts have presented carefully constructed kinetic models to account for their observed (di)methylbenzene(s) rate data. The present work represents an extension of two earlier studies[16,31] wherein compensation behavior was established for the experimentally determined aromatic hydrogenation kinetics. We believe that the "apparent" nature of experimental kinetic measurements, in general, must be recognized where corrections due to variations in surface coverage by reactants (when they occur) need to be incorporated and the kinetic and thermodynamic factors which may determine the overall reaction rate must be separated.[32] The subject matter of this paper is primarily focused on the role of hydrogen partial pressure in the hydrogenation of benzene, toluene, and the three isomeric forms of xylene over Ni/SiO_2. The kinetic data are handled using an extended power rate model which

* Corresponding author. Fax: +44 0113 2332405. E-mail: chemaak@leeds.ac.uk.
† Department of Chemical Engineering.
‡ Department of Fuel and Energy.

10.1021/ie980540t CCC: $18.00
Published on Web 02/17/1999

takes account of the inherent pressure and temperature dependences of the associated rate parameters. The adsorption coefficients of both the aromatic and hydrogen reactants under reaction conditions are extracted from the kinetic data to evaluate "catalytically significant" heats of adsorption. Reproducible turnover frequencies are provided, thermodynamic limitations are evaluated, the relationship between hydrogenation rate and heat of adsorption of hydrogen is quantified, compensation behavior is addressed, and representative global rate expressions are derived which adequately account for the observed variation of turnover frequency with temperature.

Experimental Section

A 1.5% w/w Ni/SiO_2 catalyst was prepared by homogeneous precipitation/deposition and characterized as described in detail in earlier reports.[16,33] The hydrated catalyst precursor was activated (particle diameter = 125−150 μm) by heating in a 150 cm^3 min^{-1} stream of dry hydrogen at a fixed rate of 5 K min^{-1} to a final temperature of 773 ± 1 K, which was maintained for 18 h. The activated solid is estimated to support 1.1×10^{20} exposed nickel metal sites/g of catalyst. All of the catalytic reactions were carried out under atmospheric pressure in a fixed-bed glass reactor (i.d. = 15 mm) in the temperature range 393 K ≤ T ≤ 523 K. The reactor has been described in detail elsewhere,[16] but some pertinent features are given below. A Sage pump (model 341 B) was used to deliver the aromatic feed via a syringe at a fixed rate which had been carefully calibrated, and the aromatic vapor was carried through the catalyst bed in a stream of dry hydrogen. Catalytic measurements were made at an overall space velocity equal to 2×10^3 h^{-1} and W/F values in the range of 42−112 g mol^{-1} h where W is the weight of the activated catalyst and F is the flow rate of aromatic. Mole percent conversion was kept below 25% by varying W in order to minimize heat- and mass-transfer effects. Indeed, the effectiveness factor, calculated using the approach proposed by Ruthven,[34] was consistently greater than 0.99, and heat transport effects can be disregarded when applying the criteria set down by Mears.[35] In an earlier study[16] the same reactor and reaction system was shown experimentally to operate with negligible external or internal concentration gradients under the stated experimental conditions. The reaction order with respect to hydrogen was determined, at a constant aromatic pressure (0.04 atm), by varying the hydrogen partial pressure from 0.19 to 0.96 atm using dry nitrogen as the diluent. The reaction order with respect to the five aromatic reactants was measured at a constant hydrogen pressure (0.94 atm) where the pressure of each aromatic was varied in the range 0.01−0.06 atm, again employing nitrogen as the makeup gas. All of the activity data presented in this paper were obtained at steady state and represent the average of at least five separate test samples; rate reproducibility was better than ±5%. Catalyst deactivation was probed by ascending and subsequent descending reaction temperature sequences over the entire temperature interval that was considered. In addition, two well-defined standard experiments (C_6H_6 and p-$C_6H_4(CH_3)_2$ hydrogenation at 463 and 443 K, respectively, where $P_{aromatic} = 0.04$ atm and $P_{hydrogen} = 0.96$ atm) were routinely repeated to ensure that the catalyst had not deactivated; all of the data presented in this paper were obtained in the absence of any appreciable deactivation. Product analysis was made using a Varian 3400 GC chromatograph equipped with a flame ionization detector and employing a 5% Bentone/5% diisodecyl phthalate on Chromosorb W and 30% Silicone SF96 on a 60/80 mesh acid-washed Chromosorb W (6 ft. × $^1/_8$ in.) stainless steel column for the benzene/toluene and xylene(s) reactions, respectively; data acquisition and analysis was performed using the GC Star Workstation. The overall level of hydrogenation was converted to mole percent hydrogenation using a 20-point calibration plot for each aromatic feed. The benzene/toluene (99.9+%) and xylene(s) (99%) reactants were thoroughly degassed by purging with purified helium followed by a series of freeze/pump/thaw cycles and were stored over activated molecular sieve type 5A.

Results and Discussion

Hydrogenation Results. The hydrogenation of benzene, toluene, and the xylenes over Ni/SiO_2 yielded the respective saturated cycloparaffins as the only detected products; no partially hydrogenated intermediates were isolated in the product stream. Moreover, no internal isomerization of the individual xylenes was observed, and hydrogenation generated mixtures of cis and trans stereoisomeric forms of the corresponding dimethylcyclohexane (DMC) product. The rates quoted in this paper for the conversion of the xylenes represent the overall or combined rates (for both cis and trans formation), and the effects of process variables on stereoselectivity are considered in more detail elsewhere.[31] Passage of each aromatic in a stream of hydrogen over the silica support (in the absence of nickel) did not result in any measurable degree of hydrogenation. The aromatic feed underwent progressive hydrogenolysis at a reaction temperature in excess of 523 K with the result that this investigation has been limited to temperatures ≤ 523 K.

The experimentally determined turnover frequencies (TOF), the number of molecules converted per exposed nickel metal atom per second, of the five aromatic reactants increased with increasing hydrogen partial pressure at every temperature that was considered, as is illustrated in Figure 1, taking toluene as a representative reactant. Turnover frequencies likewise were raised with increasing aromatic partial pressure, as is evident from the data presented in Table 1. Salmi et al.,[26,27] in contrast, have observed a decrease in rate with increasing toluene partial pressure and attributed this effect to a competition between hydrogen and toluene for the same adsorption sites on the catalyst (Ni/Al_2O_3) surface. The noncompetitive nature of reactive aromatic/hydrogen adsorption has, however, been established for a number of catalytic systems.[8,14,16,20−22,25] The TOF values generated in this study are lower than those reported for palladium- and platinum-based catalysts[25] but of an order similar to those quoted for Ni/Al_2O_3[27] and essentially support the generally accepted order of increasing metal efficiency (Ni < Pd < Pt) in promoting aromatic ring reduction.[3] The hydrogenation rate decreased in the order benzene > toluene > p-xylene > m-xylene > o-xylene over the entire temperature interval that was studied. It is generally accepted that the presence of a methyl substituent on the benzene ring stabilizes the adsorbed π complex with the resultant introduction of a higher energy barrier for aromatic ring hydrogenation.[36] The sequence of reactivity (albeit the

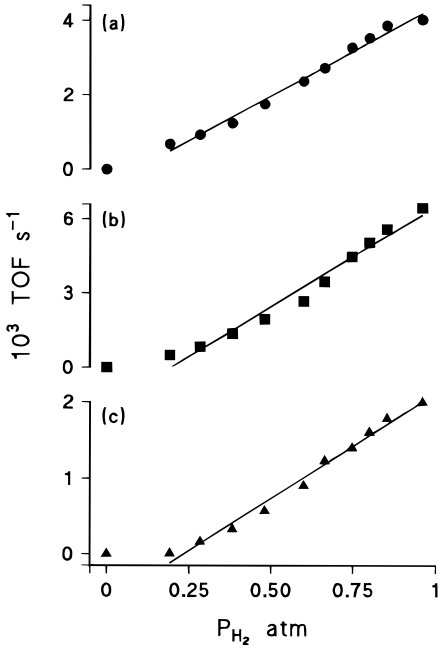

Figure 1. TOF of toluene ($P_{toluene}$ = 0.04 atm) as a function of hydrogen partial pressure at (a) 433 K (●, n = 1.2), (b) 473 K (■, n = 1.6), and (c) 523 K (▲, n = 2.3).

Table 1. Variation of the Toluene TOF with Increasing Toluene Partial Pressure at Four Representative Reaction Temperatures: $P_{Hydrogen}$ = 0.94 atm

$P_{toluene}$, atm	T, K	10^3TOF, s^{-1}
0.01	413	2.3
0.03	413	2.4
0.06	413	2.5
0.01	443	4.4
0.03	443	5.0
0.06	443	5.8
0.01	473	4.6
0.03	473	5.9
0.06	473	8.2
0.01	503	1.6
0.03	503	2.3
0.06	503	3.3

rates are similar) for the three xylene isomers can be attributed to steric effects.[31]

Application of the Power Rate Model. The reaction kinetics were modeled in the first instance using the empirical power rate model (PRM) given as

$$\mathrm{TOF} = k_{exp} P_{aromatic}{}^{m} P_{hydrogn}{}^{n} \qquad (1)$$

where k_{exp} represents the experimentally determined rate constant, $P_{aromatic}$ and $P_{hydrogen}$ are the inlet gas-phase partial pressures of the aromatic and hydrogen reactants, and m and n are the orders of the reaction with respect to the aromatic and hydrogen partial pressures, respectively. The three parameters of this model (k_{exp}, m, and n) were determined by multiple regression analysis, and representative (52 data points in each set) experimental turnover frequencies are compared in Figure 2 with the values calculated using eq 1. The quality of the fit of the PRM to the experimental data is evidenced by the slope of unity (1.0 ± 0.024) and correlation coefficients ≥ 0.994. The values of n increased from 0.8 to 2.3 as the reaction temperature was raised from 408 to 523 K. There is a linear relationship (correlation coefficient > 0.988), illustrated

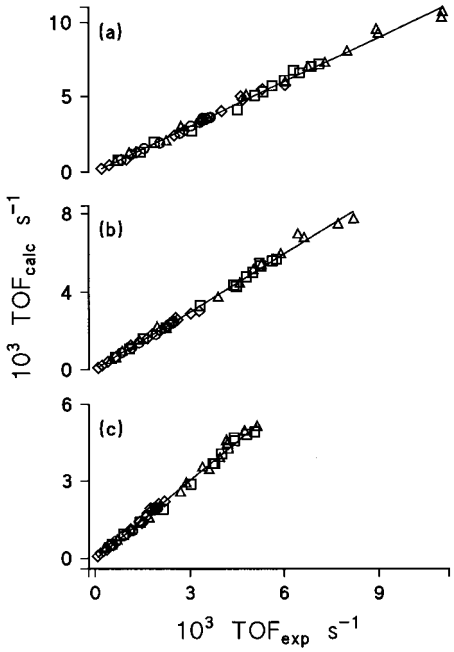

Figure 2. Comparison of experimental turnover frequencies (TOF_{exp}) with values calculated (TOF_{calc}) using the power rate model given in eq 1 for the hydrogenation of (a) benzene, (b) toluene, and (c) *m*-xylene at 413 (○), 443 (□), 473 (△), and 503 K (◇).

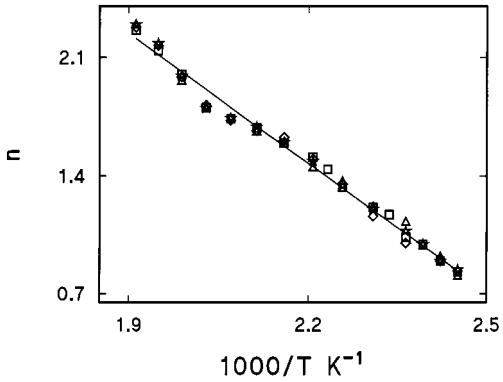

Figure 3. Linear dependence of the hydrogen partial pressure reaction order (n) on reciprocal reaction temperature for the hydrogenation of benzene (△), toluene (○), *o*-xylene (□), *m*-xylene (◇), and *p*-xylene (☆): $P_{aromatic}$ = 0.04 atm; the line represents the equation (with 95% confidence limits) $n = (-2553 \pm 69)/T + 7.1 \pm 0.2$.

in Figure 3, between the value of the exponent, n, and the reciprocal reaction temperature, which is independent of the nature of the aromatic reactant. The latter observation is taken to be diagnostic of a noncompetitive adsorption of the aromatic and hydrogen reactants, an assertion that has received full treatment in an earlier paper.[16] The reaction order with respect to partial pressure of the aromatic likewise increased (from 0 to 0.5) over the same temperature range, and the relationship between m and $1/T$ is represented by a single line in Figure 4. An increasing aromatic reaction order has been reported previously[16,27] and was attributed to a temperature-induced loss of reactive aromatic from the catalyst surface. Salmi et al., on the other hand, have recorded[26] increasingly negative values for the reaction order in toluene using a commercial alumina-supported nickel catalyst as opposed to increasingly positive values generated using a laboratory-prepared nickel−alumina system in processing toluene (from −0.4 to 0, ref 27),

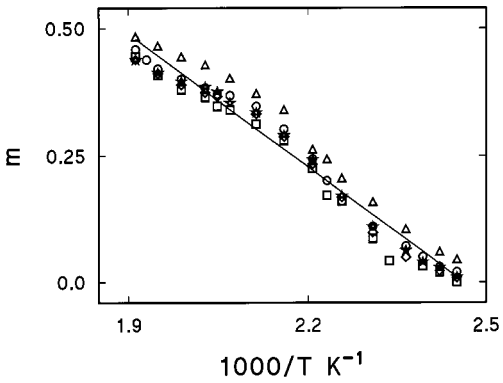

Figure 4. Linear dependence of the aromatic partial pressure reaction order (m) on reciprocal reaction temperature for the hydrogenation of benzene (△), toluene (○), *o*-xylene (□), *m*-xylene (◇,) and *p*-xylene (☆): $P_{\text{hydrogen}} = 0.94$ atm; the line represents the equation (with 95% confidence limits) $m = (-872 \pm 38)/T + 2.2 \pm 0.1$.

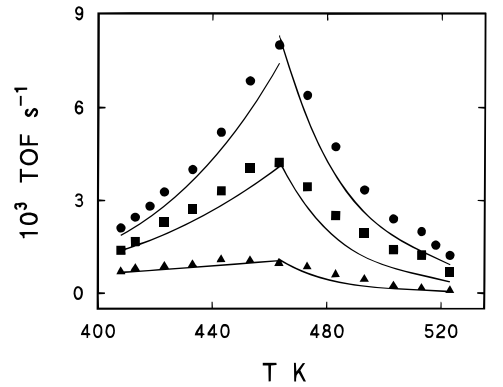

Figure 5. Variation of the TOF of toluene with reaction temperature at a partial pressure of hydrogen equal to 0.96 (●), 0.66 (■), and 0.19 atm (▲) where $P_{\text{toluene}} = 0.04$ atm: the lines represent the calculated TOF values obtained using the rate expression given in eq 9.

o-xylene (from −0.3 to 0.3, ref 29), and *p*-xylene (from 0 to 0.3, ref 29). Such an apparent incongruity serves to illustrate the inherent complexity of these systems and the difficulties involved in drawing meaningful comparisons between reports that originate from different laboratories. In this study, there is a discernible trend of increasing values of m for the five aromatic systems at a particular temperature, i.e., *o*-xylene ≤ *m*-xylene ≤ *p*-xylene < toluene < benzene, which in turn represents a decreasing degree of interaction with the catalyst surface and the observed sequence of increasing reactivity.

The turnover of each aromatic reached a maximum with increasing temperature, as has been observed elsewhere[6,8,14−16,19,25,26,29,31] and is depicted in Figure 5 for the conversion of toluene at three partial pressures of hydrogen. In general terms, such maxima ($T_{\max}$) may be attributed to catalyst poisoning or the influence of diffusion or thermodynamic limitations. Ascending and subsequent descending temperature sequences over the entire temperature interval revealed that such maxima were entirely reversible and the contribution of catalyst poisoning to such a phenomenon can be discounted. In addition, the catalytic reactor has been shown to operate with negligible mass transport/diffusion contributions to the overall rate.[16] The possibility of nickel crystallite growth during catalysis may also be rejected as the metal dispersion before and after catalyst use was essentially the same, i.e., 0.73 ± 0.05. Passage of each saturated cycloparaffin product in a stream of hydrogen over the catalyst at the optimum hydrogenation temperature did not result in any detectable dehydrogenation activity with the result that the source of $T_{\max}$ cannot be ascribed to a reverse reaction. The possibility of thermodynamic limitations was also considered, and equilibrium constants (K_p) for each gas-phase hydrogenation were determined using thermodynamic data available in the literature.[37] The temperature dependences of the associated equilibrium constants are given in Table 2. Using these relationships, the equilibrium product/reactant ratios were calculated at representative temperatures and the resultant conversion values under equilibrium conditions are compared to those generated via the catalytic hydrogenation of benzene, toluene, and *o*-xylene in Figure 6. In each case, gas-phase thermodynamic considerations predict a decrease in the equilibrium conversion as the temperature is raised. It is immediately apparent that the experimental catalytic conversions are far removed (at $T_{\max}$) from the equilibrium values and the observed temperature-related activity maxima can be attributed to surface phenomena.

In the gas-phase hydrogenation of each aromatic, equilibria between the free and complexed (or chemisorbed) reactants exist where hydrogen and the aromatic (A) adsorb on separate sites,[16,31] denoted here as S and S′, respectively.

$$\text{A(g)} + \text{S} \overset{K_A}{\rightleftharpoons} \text{A–S} \tag{2}$$

$$\text{H}_2\text{(g)} + 2\text{S}' \overset{K_H}{\rightleftharpoons} 2\text{H–S}' \tag{3}$$

The dissociative character of hydrogen adsorption on transition metals is well established while an associative adsorption of aromatic is generally accepted.[21,30,38] These adsorbed reactants can be considered to be in equilibrium with a surface activated complex (H−A−S′ or A−H−S), which in effect represents a transition state, and the equilibrium can be characterized by the constant K_{AH}, where

$$\text{A–S} + \text{H–S}' \overset{K_{AH}}{\rightleftharpoons} \text{A–H–S*} \tag{4}$$

We assume that the equilibrium constant is the same for the formation of the activated complex at site S or S′. A third site, distinct from S and S′, may well be involved in the formation of the activated complex, but for the sake of simplicity, K_{AH} can be considered to be a global equilibrium constant that relates the equilibrium concentration of the activated complex (which we denote as A−H−S*) to the equilibrium surface concentration of its components. Moreover, a variety of chemisorbed species can exist on the surface, but only one is taken to govern the rate of reaction. The hydrogenation of benzene in heterogeneous systems has been viewed as occurring via the sequential addition of hydrogen atoms to the adsorbed aromatic.[10,21,25,39] The destabilization of the aromatic resonance energy due to the addition of hydrogen atom(s) can be considered to represent the reaction energetics requirement. While the adsorbed species has been proposed to still retain appreciable aromatic character up to the addition of the third hydrogen atom pair,[40] there is persuasive evidence in the literature[25,39,41] that the addition of the first hydrogen atom is rate determining. The rate of hydrogenation follows immediately from the concentration at the

Table 2. Temperature Dependences of the Calculated Equilibrium Constants (K_p) for the Five Gas-Phase Aromatic Hydrogenation Reactions: $\log K_p = a_1/T - a_2/T^2 - a_3$, 373 K $\leq T \leq$ 600 K

reactant	product	a_1	a_2	a_3
benzene	cyclohexane	12 025.4	191 375.9	21.034
toluene	methylcyclohexane	11 733.8	155 536.1	21.018
o-xylene	*cis*-1,2-dimethylcyclohexane	11 009.4	148 139.0	21.099
	trans-1,2-dimethylcyclohexane	11 310.4	130 528.7	21.124
m-xylene	*cis*-1,3-dimethylcyclohexane	11 430.6	125 427.2	21.339
	trans-1,3-dimethylcyclohexane	11 050.0	134 317.9	21.097
p-xylene	*cis 1,4*-dimethylcyclohexane	11 038.0	125 205.8	21.047
	trans-1,4-dimethylcyclohexane	11 350.7	106 980.1	21.202

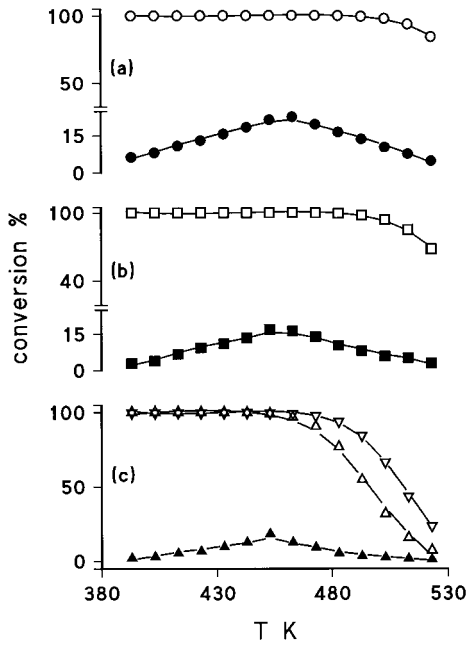

Figure 6. Equilibrium (open symbols) and catalytic (solid symbols) conversions as a function of temperature for the gas-phase hydrogenation of (a) benzene, (b) toluene, and (c) *o*-xylene (△, conversion to *cis*-1,2-dimethylcyclohexane; ▽, conversion to *trans*-1,2-dimethylcyclohexane): $P_{aromatic} = 0.04$ atm; $P_{hydrogen} = 0.96$ atm.

surface of this so-called rate-determining complex according to

$$\mathrm{TOF} = k_{true}[\mathrm{A{-}H{-}S^*}] \qquad (5)$$

where k_{true} is the rate constant for the transformation of the adsorbed complex as distinct from the experimental parameter given in eq 1. When the equilibrium constants given in eqs 2−4 are incorporated, rate expressions of the form

$$\mathrm{TOF} = k_{true}K_{AH}[\mathrm{A{-}S}][\mathrm{H{-}S'}] \qquad (6)$$

and

$$\mathrm{TOF} = k_{true}K_{AH}K_A{K_H}^{1/2}[\mathrm{A(g)}][\mathrm{H_2(g)}]^{1/2} \qquad (7)$$

result. A direct comparison of eq 7 with eq 1 affords a grouping of terms where k_{exp} is equivalent to $k_{true}K_{AH}K_A{K_H}^{1/2}$ which is in keeping with the approach proposed by Patterson and Rooney.[42] Moreover, the product of the inlet hydrogen and aromatic partial pressures ($P_{aromatic}{}^m P_{hydrogen}{}^n$) corresponds to the product of the equilibrium concentrations in the gas phase ($[\mathrm{A(g)}][\mathrm{H_2(g)}]^{1/2}$). The variation with temperature of the experimentally determined *m* and *n* exponents therefore reflects the variations in the equilibrium gas-phase partial pressures. These experimental reaction orders do not refer to the number of molecules involved in the chemical transformation, i.e., do not define the composition of the surface activated complex, but merely reflect the dependence of rate on gas-phase pressure and as such should be termed "apparent" rather than "true" reaction orders. They are, however, useful in that they reveal the temperature-induced changes in the adsorption of the reactive species. During catalysis, the equilibria given in eqs 2−4 are established, but an increase in temperature must displace the relative proportions of the participating species involved in surface interconversions in the direction of decreasing surface coverage through desorption. The existence of a T_{max} must then arise because of combined but opposing temperature dependences of the rate constant for the surface reaction (k_{true}) and the equilibrium adsorption constants ($K_A K_H{}^{1/2} K_{AH}$) where the increase in rate constant is overcompensated by a decrease in the adsorption constants, and the latter effect is reflected in the temperature dependences of *m* and *n*.

The power rate model can be extended to include the apparent activation energy (E_{app}) and the associated preexponential (frequency) factor (k_0)

$$\mathrm{TOF} = k_0 \exp\left(\frac{-E_{app}}{RT}\right) P_{aromatic}{}^m P_{hydrogen}{}^n \qquad (8)$$

where each system is characterized by two values of E_{app} and k_0 for $T \leq T_{max}$ and $T \geq T_{max}$. As both reaction orders (*m* and *n*) vary with temperature, such temperature dependences may be incorporated to construct a global rate expression that can be used to predict the TOF at a particular feed composition. Using the linear relationships presented in Figures 3 and 4, a rate expression common to the five aromatic reactants results

$$\ln \mathrm{TOF} = \ln k_0 + 2.2 \ln P_{aromatic} + 7.1 \ln P_{hydrogen} - \frac{1}{T}\left(\frac{E_{app}}{R} + 872 \ln P_{aromatic} + 2553 \ln P_{hydrogen}\right) \qquad (9)$$

The values for E_{app} and $\ln k_0$ are taken from previous reports[16,31] wherein the raw data and the treatment of results are recorded. The validity of this expression is assessed in Figure 5 where experimental and calculated TOFs are compared as a function of temperature. The common extended PRM expression does represent the experimental data with a reasonable degree of accuracy. The capability of a common empirical PRM expression to reproduce experimental rate data for each individual aromatic system suggests that eq 9 or any other rate expressions of this form can serve as a useful aid in reactor design. The level of agreement between experimental and calculated TOF is improved somewhat (to

within ±15%) by employing individual m vs $1/T$ correlations for each aromatic.

While the PRM is certainly flawed in that it is insensitive to the precise kinetic scheme that is involved, the extended corrected form does provide a solid basis for representing reaction rate data over a wide range of process conditions. However, the description of the reaction rate by the PRM is only valid within the restricted range of temperatures and pressures that were considered in the experimental studies. For instance, the linear plots presented in Figure 1 do not extrapolate to the origin, and the rate expression that results cannot be applied where $P_{\text{hydrogen}} < 0.19$ atm.

Nevertheless, eq 9 does not suffer the drawback of many expressions, largely based on Langmuir−Hinshelwood formulations, where presumed constants become adjustable parameters when correlating rate data and a deal of discrimination and estimation is involved.[38] It is not surprising that, given the interrelated multivariable nature of gas-phase heterogeneous benzene hydrogenation, Mirodatos et al.[11] have called into question the feasibility of attempting to describe the reaction by one mechanism over a large range of temperature and pressure conditions. In essence, the rate expression that is generated by applying the extended PRM represents a homogeneous kinetic approach to heterogeneous systems. Heterogeneous processes, however, differ from homogeneous reactions in that not all equivalent molecules can be regarded as being equally reactive. The experimentally determined activation energies must of necessity be designated "apparent" as no provision is made for variations in the effective concentration of the adsorbed reactive species. The modifications that we have made to the general PRM given in eq 1 are essentially corrections for the temperature dependence of the gas-phase pressure requirements which do reflect surface concentration variations but do not deliver values for the true rate constant. Rather, a composite term results that incorporates the equilibrium constants given in eq 7.

Meaningful use of experimentally determined activation energies reported for heterogeneous systems is accordingly problematic. Moreover, it is fair to state that a large proportion of the published kinetic reports are characterized by incomplete procedural descriptions where information on pertinent catalyst physical features, reactant(s) pressures (total and partial, presence/absence of diluents), contact time (presence/absence of mass/heat-transfer effects), space velocities, contributions due to catalyst deactivation, use of initial/steady-state rates, and degree of accuracy/data reproducibility, is often missing or difficult to extract. As a means of illustrating the difficulties involved in comparing kinetic data, the reported activation energies for the hydrogenation of benzene have, in many instances, been generated from the temperature dependences of the reaction rate rather than the rate constant[5,6,8] while in a number of reports it is unclear how the quoted activation energy was derived.[4,7,9−11] The activation energy generated from rate constants will only equal that obtained from the use of raw rate data when the reaction orders are temperature invariant. This is not the case with the systems under consideration, and the differences in values are marked, as is evident from the information provided in Table 3. The activation energies derived directly from TOF values and likewise the frequency factors are consistently lower than the values generated from the Arrhenius treatment of rate constants. Such an appreciable modification of the data that is induced by incorporating corrections due to the temperature-related variations in the gas-phase partial pressure dependences really calls into question the validity of employing as a basis for comparison activation energy data that are not generated or determined under "standard" or "reference" conditions.

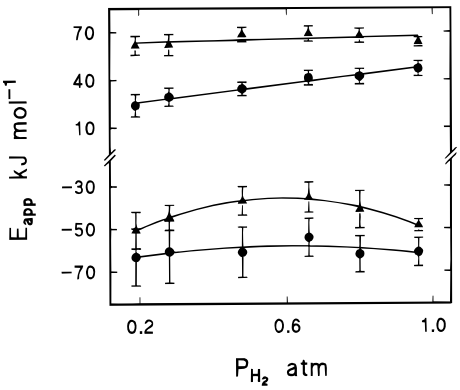

Figure 7. Apparent activation energies (E_{app}) for the hydrogenation of toluene as a function of hydrogen partial pressure in the two regions where $T \leq T_{max}$ (positive values) and $T \geq T_{max}$ (negative values): E_{app} values are generated from the temperature dependence of TOF (●) and the rate constant (▲).

Table 3. Comparison of the Apparent Activation Energies with 95% Confidence Limits (E_{app}, kJ mol^{-1}) and Preexponential Factors (k_0) Generated from Arrhenius Relationships Employing Turnover Frequencies (s^{-1}) or Rate Constants (s^{-1}) atm$^{-(m+n)}$) as the Rate Parameter: for TOF Data, $P_{\text{hydrogen}} = 0.96$ atm and $P_{\text{aromatic}} = 0.04$ atm

		rate parameter			
		k, s^{-1} atm$^{-(m+n)}$		TOF s^{-1}	
aromatic reactant	T range, K	k_0	E_{app}	k_0	E_{app}
benzene	393−473	8×10^3	49.2 ± 2.0	16	29.1 ± 2.4
	473−523	3×10^{-6}	−35.9 ± 2.3	6×10^{-8}	−47.0 ± 4.5
toluene	388−463	3×10^5	63.6 ± 2.9	2×10^3	46.9 ± 4.7
	463−523	7×10^{-8}	−48.6 ± 2.9	1×10^{-9}	−61.1 ± 6.6
o-xylene	393−453	4×10^6	73.4 ± 3.8	2×10^4	56.6 ± 3.3
	453−523	2×10^{-9}	−60.5 ± 3.0	1×10^{-10}	−67.5 ± 2.5
m-xylene	393−453	1×10^6	68.1 ± 3.4	7×10^3	52.2 ± 2.7
	453−523	6×10^{-9}	−56.1 ± 3.3	4×10^{-10}	−63.2 ± 4.2
p-xylene	393−453	4×10^5	64.9 ± 2.6	4×10^3	49.7 ± 2.5
	453−523	3×10^{-8}	−49.6 ± 3.2	8×10^{-10}	−60.8 ± 3.9

Compensation Behavior. From a consideration of the parameters included in eq 9, the discrepancy between the experimental and calculated temperature dependences of TOF in Figure 5 (which is evident for each aromatic system) may be attributed to variations in E_{app} and ln k_0 with changes in the partial pressure of hydrogen. Certainly, in gas-phase hydrogenolysis systems, the experimentally determined activation energies have been shown to be a function of the reaction order with respect to hydrogen[43] and the gas-phase hydrogen partial pressure[23,32] while Coenen et al.[4] have observed an increase in E_{app} with increasing P_{hydrogen} in the liquid-phase hydrogenation of benzene. In this study of gas-phase hydrogenation processes, the apparent activation energy (and the associated preexponential factor) was also found to be pressure dependent, as is illustrated in Figure 7, once again taking the conversion of toluene as representative of the five aromatic systems. In essence, there is no single value of E_{app} or ln k_0 which can truly serve to characterize the system over the stated range of hydrogen partial pressures. It may be

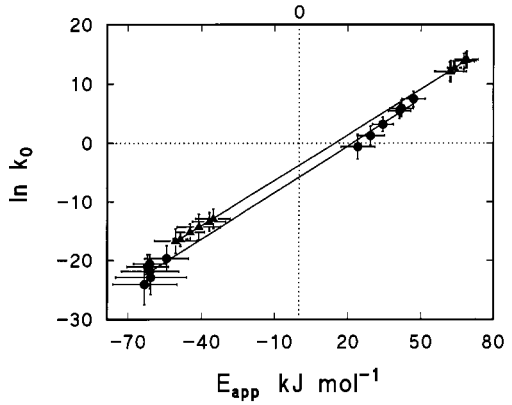

Figure 8. Compensation plot for the hydrogenation of toluene where the data are generated by varying the partial pressure of hydrogen and are based on TOF (●, equation of the fitted line is $\ln k_0 = (0.2652 \pm 0.0132)E_{app} - 5.7710 \pm 0.6621$) and rate constant, k, values (▲, equation of the fitted line is $\ln k_0 = (0.2582 \pm 0.00132)E_{app} - 3.7486 \pm 0.0701$).

noted that the E_{app} values generated from TOF data are more sensitive to changes in the hydrogen partial pressure. An incorporation of corrections due to the effect of changes in pressure on E_{app} and $\ln k_0$ was found to further lower the deviation of the predicted from the observed TOFs (to ±8%) but results in very cumbersome rate expressions, shown below for $T \leq T_{max}$

$$\ln \text{TOF} = [14.6P_{\text{hydrogen}} - 11.7(P_{\text{hydrogen}})^2 + 9.5] + 2.4 \ln P_{\text{toluene}} + 7.1 \ln P_{\text{hydrogen}} + \frac{1}{T}\{[-6567P_{\text{hydrogen}} + 5283(P_{\text{hydrogen}})^2 - 6238] - 967 \ln P_{\text{toluene}} - 2553 \ln P_{\text{hydrogen}}\} \quad (10)$$

The improvement in the fit to the experimental data is insufficient to warrant these additional corrections to eq 9 particularly for design purposes.

Nevertheless, this variance of E_{app} with process conditions suggests the likelihood of a compensation effect which is manifest in a linear relationship between E_{app} and $\ln k_0$,[44] where

$$\ln k_0 = c_1 E_{app} + c_2 \quad (11)$$

and c_1 and c_2 are constants. Such a sympathetic variation of the frequency factor and the apparent activation energy for the hydrogenation of toluene is illustrated in Figure 8 where the compensation behavior is the direct consequence of variations in the partial pressure of hydrogen. Strict adherence to the compensation equation (eq 11) requires all associated $\ln k$ vs $1/T$ plots to intersect at a common isokinetic temperature (T_{iso}) where

$$T_{iso} = (c_1 R)^{-1} \quad (12)$$

The computed isokinetic temperature generated from the data presented in Figure 8 is 466 ± 2 K, which is in good agreement with the values quoted in earlier studies.[16,31] The latter reports focused on the role of each aromatic in determining hydrogenation kinetics where the observed compensation behavior is attributed to apparent kinetic measurements wherein the E_{app} and k_0 terms incorporate contributions due to the temperature dependences of the surface concentration of adsorbed reactive species. The appearance of compensation

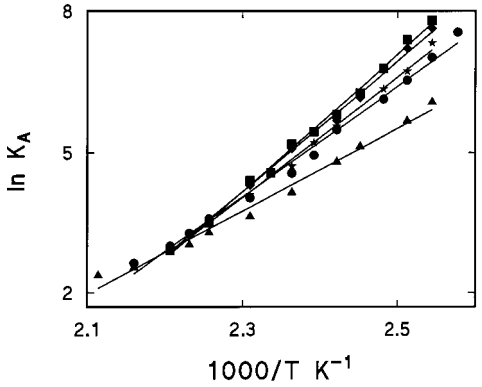

Figure 9. Variation of the aromatic adsorption equilibrium constant (derived from kinetic data) with temperature for the hydrogenation of benzene (▲, $\Delta H = -74$ kJ mol^{-1}), toluene (●, $\Delta H = -98$ kJ mol^{-1}), *o*-xylene (■, $\Delta H = -121$ kJ mol^{-1}), *m*-xylene (◆, $\Delta H = -116$ kJ mol^{-1}), and *p*-xylene (★, $\Delta H = -107$ kJ mol^{-1}): $P_{\text{hydrogen}} = 0.94$ atm.

behavior due solely to variations in the partial pressure of hydrogen where the data is treated using the PRM approach indicates that the phenomenon is not due to the imposition of a particular reaction model. Rather, the compensation effect arises because of the contribution P_{hydrogen} makes to surface coverage by reactive hydrogen. Compensation behavior is likewise observed when TOFs are used to generate E_{app} and $\ln k_0$ values where the inferred T_{iso} (454 ± 23 K) is characterized by a wider margin of uncertainty but concurs with the value determined from the rate constants.

Catalytically Significant Heats of Adsorption. (i) Aromatic Adsorption. The temperature dependence of the experimental exponents, m and n, reflects the changes in the surface concentration(s) of the reactive species. From a consideration of eqs 1 and 6, the fractional coverage (θ_A) of sites S as a function of temperature can be approximated by the changes to the term $P_{\text{aromatic}}{}^m$ over the range of partial pressures that were studied, where

$$\theta_A = \frac{K_A P_{\text{aromatic}}}{1 + K_A P_{\text{aromatic}}} \quad (13)$$

When the aromatic and hydrogen reactants are taken to adsorb noncompetitively and the standard Langmuir adsorption relationship is applied, the adsorption equilibrium constant (K_A) was evaluated where $T \leq T_{max}$. The associated van't Hoff plots are given in Figure 9, and the computed heats of adsorption are recorded in the figure caption. The heats of adsorption of each aromatic were independent (within the 95% confidence band) of the aromatic partial pressure in the range of pressures considered in this study. The sequence of increasing $-\Delta H_{ads}$ values mirrors exactly that of decreasing reactivity and is indicative of an associative π-bonding adsorbate/adsorbent interaction in generating the surface reactive aromatic. This sequence of sorption energies finds qualitative agreement with Pope's[45] studies of aromatic adsorption on ZSM-5 and silicalite. Isolated heats of adsorption, by that we mean measurements made in the absence of any catalytic transformations, are available in the literature. Benzene adsorption on zeolites has yielded values in the range of −50 to −75 kJ mol^{-1},[36,45] while adsorption on nickel metal varies from −50[46] to −105 kJ mol^{-1} at monolayer coverage.[47] Indeed, heats of aromatic adsorption have

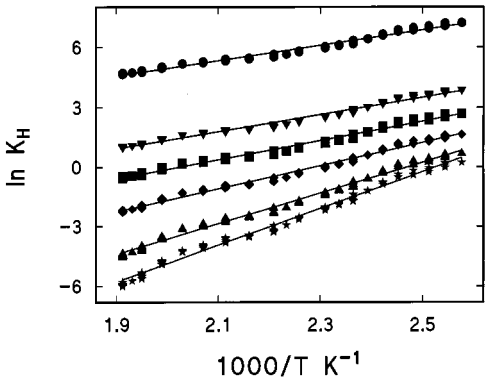

Figure 10. Variation of the adsorption equilibrium constant of hydrogen with temperature in the hydrogenation of the five aromatic reactants where $P_{hydrogen}$ = 0.96 (●), 0.80 (▼), 0.66 (■), 0.48 (◆), 0.28 (▲), and 0.19 atm (★): $P_{aromatic}$ = 0.04 atm.

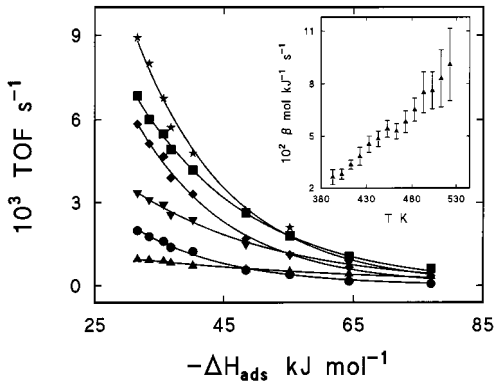

Figure 11. Relationship between TOF and the heat of adsorption of hydrogen (ΔH_{ads}) where the solid lines represent the expression TOF = $\alpha \exp(-\beta \Delta H_{ads})$ for the hydrogenation of benzene at 473 K (★, $\alpha = 7.57 \times 10^{-2} \pm 2.27 \times 10^{-2}$, $\beta = 6.81 \times 10^{-2} \pm 8.49 \times 10^{-3}$) and 493 K (◆, $\alpha = 5.31 \times 10^{-2} \pm 1.30 \times 10^{-2}$, $\beta = 7.00 \times 10^{-2} \pm 6.90 \times 10^{-3}$) and the hydrogenation of toluene at 393 K (▲, $\alpha = 2.16 \times 10^{-3} \pm 3.03 \times 10^{-4}$, $\beta = 2.60 \times 10^{-2} \pm 3.49 \times 10^{-3}$), 453 K (■, $\alpha = 4.02 \times 10^{-2} \pm 4.53 \times 10^{-3}$, $\beta = 5.65 \times 10^{-2} \pm 3.11 \times 10^{-3}$), and 513 K (●, $\alpha = 1.79 \times 10^{-2} \pm 6.03 \times 10^{-3}$, $\beta = 6.95 \times 10^{-2} \pm 9.49 \times 10^{-3}$) and the hydrogenation of *o*-xylene at 433 K (▼, $\alpha = 1.41 \times 10^{-2} \pm 2.49 \times 10^{-3}$, $\beta = 4.53 \times 10^{-2} \pm 4.63 \times 10^{-3}$): $P_{aromatic}$ = 0.04 atm. Inset: The variation of the variable β with temperature for the hydrogenation of *o*-xylene where the error bars represent 95% confidence limits.

been shown, in general, to depend on the surface coverage.[45,46] Toluene adsorption on zeolites[45] has, in turn, generated values in the range of −50 to −80 kJ mol^{-1}, which are comparable to or lower than the spread of values (−50 to −90 kJ mol^{-1}) quoted for xylene(s).[45,48] Directly measured adsorption enthalpies differ appreciably in magnitude from the values extracted from kinetic studies, as has been well demonstrated by Tétényi[39] for the adsorption of benzene on Pt black. Values in the range of −59 to −71 kJ mol^{-1} inferred from benzene hydrogenation kinetics on supported palladium[49] seem to be in line with the direct adsorption methods while values of −29 to −54 kJ mol^{-1} quoted for the platinum-promoted hydrogenation of toluene[50] seem low by comparison. Likewise the values of −30 to −40 kJ mol^{-1} on supported nickel obtained from a kinetic model for *o*- and *p*-xylene[30] appear to be on the low side as too is the value of −60 kJ mol^{-1} extracted by the authors from the temperature-related adsorption equilibrium constants tabulated in ref 27. The heats of adsorption extracted from the kinetic treatment in this study seem somewhat high when compared with the values quoted above. The adsorption enthalpies are certainly greater in magnitude than the associated heats of condensation[51] for the ideal aromatic gas whether the phase change is taken to be from gas to liquid (−37 kJ mol^{-1} for *o*-xylene) or from gas to solid (−43 kJ mol^{-1} for *o*-xylene) which is certainly indicative of chemisorption on the surface. The heats of adsorption that are derived from our kinetic data refer to the surface-adsorbed aromatic species that is transformed to the saturated product and, as such, represent the "catalytically significant" heats of adsorption.

(ii) Hydrogen Adsorption. Where hydrogen adsorbs dissociatively on sites S′, the change with temperature of the concentration of surface reactive hydrogen, characterized by K_H, may also be evaluated from the variations in the term $P_{hydrogen}{}^n$. The variation of K_H with temperature is illustrated graphically in Figure 10 where the slopes of the lines yield values of ΔH_{ads}. The K_H values for the five processes fall on the same line, again indicative of noncompetitive adsorption, and give heats of adsorption of hydrogen that increase in magnitude with decreasing $P_{hydrogen}$ in the range of −31 to −77 kJ mol^{-1}, which represent overall surface coverages varying from 0.02 to 0.97. The values of K_H are appreciably lower than those recorded for K_A, as has been reported previously for palladium systems.[25] As in the case of the aromatic adsorption data, the ΔH_{ads} values quoted in this paper reflect only the hydrogen participating in each reaction, the "catalytically significant" energetics, and can differ appreciably from the heats of adsorption measured in the absence of any surface reaction(s). Indeed, calorimetric and TPD studies of hydrogen adsorption on nickel have yielded enthalpies in the overall range of −40 to −120 kJ mol^{-1}.[52,53] It is now recognized that different forms of hydrogen, with different degrees of interaction, are present on the surface of nickel catalysts[17,54] with reported adsorption enthalpies ranging from −110 to in excess of −400 kJ mol^{-1}.[54] The data generated in this study suggest that weakly interacting hydrogen is the reactive surface species and the inferred energetics agree with the value of −30 kJ mol^{-1} quoted by Mirodatos et al.[11] in their steady-state study of benzene hydrogenation on unsupported nickel and Ni/SiO_2 catalysts. Smeds et al., in contrast, have derived ΔH_{ads} values of −50 to −60[30] and −104 kJ mol^{-1} [26] from their kinetic studies of *o*- and *p*-xylene and toluene hydrogenation, respectively, over Ni/Al_2O_3. The variation of TOF with ΔH_{ads} can be represented by an expression of the form

$$\text{TOF} = \alpha \exp(-\beta \Delta H_{ads}) \qquad (14)$$

where α is a constant and β can be considered to reflect the dependence of the specific rate on the heat of adsorption of hydrogen; typical data with the requisite fits are presented in Figure 11. An increase in the strength of chemisorption of hydrogen can be said to inhibit the specific rate of hydrogenation. This result finds qualitative support in the observation that the weakly bound surface hydrogen is active in the hydrogenation of benzene.[4,17] The response of the variable β to increases in the reaction temperature is illustrated in the inset of Figure 11. The dependence of rate on the degree of interaction of hydrogen with the surface is markedly greater at the higher reaction temperatures presumably because of a greater contribution of weakly chemisorbed hydrogen to the reduction of the adsorbed aromatic. While the presence of the supported nickel

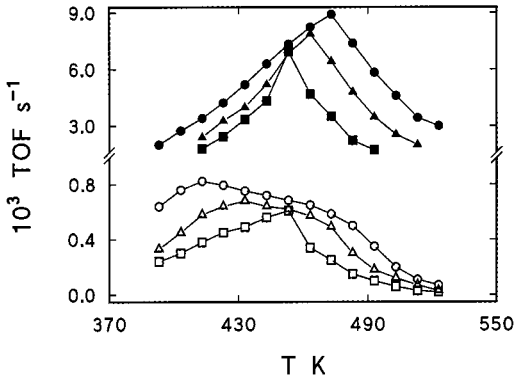

Figure 12. Hydrogenation of benzene (○, ●), toluene (△, ▲), and *o*-xylene (□, ■) at $P_{hydrogen}$ = 0.96 atm (solid symbols) and 0.19 atm (open symbols) as a function of reaction temperature: $P_{aromatic}$ = 0.04 atm.

metal is essential for the dissociative adsorption of hydrogen, weakly interacting spillover hydrogen may well represent the active hydrogenating agent. Benzene has been shown to react readily with spillover hydrogen on oxide surfaces[55] at reaction temperatures comparable to those employed in this study. Moreover, aromatic reactants are known to adsorb on oxide supports.[44,56] An earlier spectroscopic study of benzene adsorbed on NiNaY[39] revealed that the strength of interaction decreased on reducing the divalent Ni^{2+} component to Ni^0, suggesting that the aluminosilicate framework and/or charge-balancing cations rather than the supported nickel metal served as the principal site for adsorption. In terms of the notation used in this paper, S could be assigned to adsorption sites on the silica support and S′ the supported nickel metal. The metal/support interfacial region may then provide the predominant contribution to the observed activity where there is a relatively high concentration of adsorbed aromatic and hydrogen transport occurs readily, in keeping with the steps envisaged by Vannice et al.[50]

Temperature-Dependent Activity Maximum (T_{max}). Returning to the phenomenon of the appearance of a T_{max} in the TOF vs T plots, the actual value of the temperature-dependent activity maximum was found to depend on the nature of the aromatic reactant and the hydrogen partial pressure, as is best illustrated in Figure 12. While the temperature dependences of the TOFs are not as marked at lower hydrogen partial pressures, a decrease in $P_{hydrogen}$ from 0.96 to 0.19 atm resulted in a shift in T_{max} from 473 to 413 K and from 463 to 433 K for the benzene and toluene reactants, respectively. The maximum in the turnover of the three xylene isomers at 453 K was unaffected by variations in the partial pressure of hydrogen; only *o*-xylene is represented in Figure 12 for the sake of clarity. It is instructive to note that while activity for the three aromatic reactants was lower at the reduced hydrogen partial pressures, the value of T_{iso} remained constant in keeping with the observed compensation behavior. From a consideration of aromatic adsorption strength, the order of increasing T_{max} should be opposite to that observed at higher hydrogen partial pressures; i.e., the presumed stronger interaction of xylenes with the catalyst should necessitate a higher temperature to lower the surface coverage to the limiting value where reaction probability drops. At the higher values of $P_{hydrogen}$, the critical loss of the reactive form of the aromatic can be said to occur at decreasing temperatures with increasing methyl substitution. It has been speculated that benzene is not solely adsorbed on metals as a π complex but that the π-bonded species exists in equilibrium with σ- and π/σ-bonded species where the σ-bonded species inhibits hydrogenation by competitive adsorption.[10] If such σ bonding occurs during the chemisorption of toluene and the xylenes, the observed temperature-related maxima in activity at higher values of $P_{hydrogen}$ may be due to an increase in the relative coverage by an unproductive σ species. Furthermore, the introduction of a steric factor due to the presence of methyl substituent(s) may favor a nonplanar orientation of the aromatic nucleus relative to the metal surface with a consequent greater likelihood of σ bonding. Hydrogen also exists in different adsorbed forms; the more mobile dissociated hydrogen can be termed reactive while the irreversibly adsorbed component can be considered unreactive and does not take part in the reaction. Only the reactive states contribute to catalysis where, at the lower partial pressure of hydrogen corresponding to greater catalytic heats of adsorption, the surface reaction is more energetically demanding. Under these conditions the temperature dependence of the hydrogenation rate is governed by the ease of hydrogen addition to the surface reactive aromatic with a consequent sequence of T_{max} values that reflects, in essence, the reactivity of the reactive species rather than the relative abundance on the surface which is assumed to be the governing factor at higher hydrogen partial pressures. The observed temperature dependences of aromatic TOFs are the result of variations in the surface availability and reactivity of both the surface hydrogen and hydrocarbon species. In these systems, a high catalytic efficiency then results from reactants/catalyst interactions that are sufficiently strong to ensure a plentiful supply of the reactants on the surface but not too strong to fix the reactants to the surface in an unreactive form.

Catalytically Relevant Energetics. The experimentally determined activation energies do not represent the true energetics (E_{true}) involved in the transformation of the surface activated complex because of the involvement of preequilibria to the rate-determining step. The value of E_{true} can be arrived at by adding the adsorption enthalpies of those reactants whose concentration is changing,[57] which in this case leads to

$$E_{true} = E_{app} - (\Delta H_{ads}(\text{aromatic}) + \Delta H_{ads}(\text{hydrogen})) \quad (15)$$

From a consideration of the enthalpy values extracted from the data plotted in Figures 9 and 10 and the apparent activation energies reported elsewhere,[16,31] true activation energies for the five reaction systems under the stated experimental conditions are determined to be in the range of 155−272 kJ mol^{-1}. Such seemingly high values are the result of the exothermic preequilibria which serve to activate the reactants. The range of values is in reasonable agreement with previous E_{true} data quoted by the authors[16,31] where the activation energies obtained over $T \leq T_{max}$ and $T \geq T_{max}$ were taken to be equivalent to the energies of adsorption and desorption, respectively, and the catalytically significant adsorption heats were accordingly incorporated. The true activation energies extracted from eq 15 incorporate all of the catalytically significant energetics involved in the process and, as a result, are also dependent on hydrogen partial pressure as this variable serves to influence the energy of hydrogen activation

on the surface and its reactivity. From a consideration of eqs 8 and 14, an equivalent form of the compensation plot is obtained

$$\ln k_0 = \ln \alpha - m \ln P_{\text{aromatic}} - n \ln P_{\text{hydrogen}} - \beta \Delta H_{\text{ads}}(\text{hydrogen}) + E_{\text{app}}/RT \quad (16)$$

where the $\ln \alpha - \beta \Delta H_{\text{ads}}$(hydrogen) term characterizes reactivity and the $-(m \ln P_{\text{aromatic}} + n \ln P_{\text{hydrogen}})$ term the availability of surface reactants. Two terms in eq 16, i.e., $n \ln P_{\text{hydrogen}}$ and $\beta \Delta H_{\text{ads}}$(hydrogen), are dependent on both temperature and hydrogen partial pressure and, as a result, $\ln k_0$ is a composite made up of such contributions. An increase in E_{app} caused by changes to P_{hydrogen}, for example, is accompanied by an increase in $\ln k_0$ due to the interplay between the pressure-dependent terms in eq 16 which gives rise to the observed compensation behavior. This effect results from the indirect nature of the experimental approaches and the practical difficulties involved in direct measurement of the surface-controlled reaction kinetics. The experimentally determined Arrhenius parameters should be denoted as "composite frequency factors" and "composite activation energies" as this establishes more explicitly the nature of these measurements.

Conclusions

In the hydrogenation of benzene, toluene, and *o*-, *m*-, and *p*-xylene over Ni/SiO_2 where P_{hydrogen} and P_{aromatic} are varied in the ranges 0.19−0.96 and 0.01−0.06 atm, respectively, and 393 K ≤ T ≤ 523 K, the principal findings reported herein may be summarized as follows:

(i) TOF, at every temperature, increases with increasing P_{hydrogen} and P_{aromatic}.

(ii) TOF decreases in the order benzene > toluene > *p*-xylene > *m*-xylene > *o*-xylene, which, in turn, represents the order of increasing stability (and decreasing reactivity) of the adsorbed π complex.

(iii) A reversible temperature-related activity maximum (T_{max}) is observed in each system under reaction conditions that are far removed from equilibrium conversions. The values of T_{max} decrease on lowering P_{hydrogen} in the conversion of benzene and toluene, but the conversion of the three xylene isomers is characterized by a common T_{max} which remains unaffected by changes in partial pressures. Under reaction conditions, the catalyst surface is covered by reactive and unreactive species and the observed T_{max} values arise because of the temperature dependence of both the surface availability and reactivity of the active component.

(iv) An extended common power rate model that incorporates the temperature dependences of the reaction orders provides a satisfactory representation of the observed TOF vs T profiles at different values of P_{hydrogen} and is presented as a useful reactor design aid.

(v) The experimentally determined Arrhenius parameters are dependent on the hydrogen partial pressure and exhibit compensation behavior—such terms must be considered to be composites which incorporate contributions due to surface concentrations and reactivities.

(vi) Aromatic and hydrogen heats of adsorption extracted from reaction data differ markedly from enthalpy changes measured in the absence of any surface reaction(s), and the former may be considered to reflect the catalytically significant energetics. An increase in the strength of chemisorption of hydrogen inhibits the specific hydrogenation rate, and the less strongly bound hydrogen appears to be the reactive component.

Acknowledgment

The authors are indebted to Prof. G. C. Bond for his helpful comments regarding this paper.

Nomenclature

Lower Case Terms

ads = adsorption
app = apparent kinetic parameter
calc = calculated values
iso = isokinetic parameter
max = value corresponding to maximum reaction rate
obs = observed (experimental) values
true = true kinetic parameter

Upper Case Terms

m = reaction order with respect to the aromatic partial pressure
n = reaction order with respect to the hydrogen partial pressure

Greek Symbols

α = constant, s^{-1}
β = constant, mol kJ^{-1} s^{-1}
θ = fractional surface coverage

Other Terms

A = aromatic
c_1 = constant, mol $atm^{-(m+n)}$ s^{-1} kJ^{-1}
c_2 = constant, $atm^{-(m+n)}$ s^{-1}
DMC = dimethylcyclohexane
F = molar flow rate of aromatic, mol h^{-1}
(g) = gas phase
ΔH = heat of adsorption, kJ mol^{-1}
k = rate constant, $atm^{-(m+n)}$ s^{-1}
k_0 = preexponential factor, $atm^{-(m+n)}$ s^{-1}
K_A = aromatic adsorption equilibrium constant
K_{AH} = equilibrium constant for the formation of the activated complex
K_H = hydrogen adsorption equilibrium constant
K_p = equilibrium reaction constant, atm^{-3}
PRM = power rate model
P = partial pressure, atm
R = universal gas constant, 8.314 J mol^{-1} K^{-1}
S = aromatic adsorption site
S′ = hydrogen adsorption site
T = temperature, K
TOF = turnover frequency, s^{-1}
W = weight of catalyst, g

Literature Cited

(1) Satterfield, C. N. *Heterogeneous Catalysis in Practice*; McGraw-Hill: New York, 1980.

(2) Stanislaus, A.; Cooper, B. H. Aromatic Hydrogenation Catalysis—A Review. *Catal. Rev.−Sci. Eng.* **1994**, *36*, 75.

(3) Rylander, P. N. *Hydrogenation Methods*; Academic Press: London, 1985.

(4) Coenen, J. W. E.; van Meerten, R. Z. C.; Rijnten, H. Th. Dependence of Activity for Benzene Hydrogenation of Nickel on Crystallite Size. In *Proceedings of the 5th International Congress on Catalysis*; Hightower, J. W., Ed.; North-Holland: Amsterdam, The Netherlands, 1973; p 671.

(5) Germain, J. E.; Maurel, R.; Bourgeois, Y.; Sinn, R. Kinetics of the Gas Phase Hydrogenation of Benzene. 1. Orders with Respect to Benzene and Hydrogen. *J. Chim. Phys.* **1963**, *60*, 1219.

(6) Nicolai, J.; Martin, R.; Jungers, J. C. Kinetics of Benzene Hydrogenation. *Bull. Soc. Chim. Belg.* **1948**, *57*, 555.

(7) Aben, P. C.; Platteeuw, J. C.; Southame, B. The Hydrogenation of Benzene over Supported Platinum, Palladium and Nickel Catalysts. In *Proceedings of the 4th International Congress on Catalysis*; Hightower, J. W., Ed.; North-Holland: Amsterdam, The Netherlands, 1969; p 395.

(8) van Meerten, R. Z. C.; Coenen, J. W. E. Gas Phase Hydrogenation on a Nickel−Silica Catalyst. 1. Experimental Data and Phenomenological Description. *J. Catal.* **1975**, *37*, 37.

(9) Dixon, G. M.; Singh, K. Catalysis over Coprecipitated Nickel/Alumina. *Trans. Faraday Soc.* **1969**, *65*, 1128.

(10) Prasad, K. H. V.; Prasad, K. B. S.; Mallikarjunan, M. M.; Vaidyeswaren, R. Self-Poisoning and Rate Multiplicity in Hydrogenation of Benzene. *J. Catal.* **1983**, *84*, 65.

(11) Mirodatos, C.; Dalmon, J. A.; Martin, G. A. Steady-State and Isotopic Transient Kinetics of Benzene Hydrogenation on Nickel-Catalysts. *J. Catal.* **1987**, *105*, 405.

(12) Zlotina, N. E.; Kiperman, S. L. On the Kinetics of Benzene Hydrogenation on Nickel Catalysts in a Gradient Free System. *Kinet. Katal.* **1967**, *8*, 337.

(13) van Meerten, R. Z. C.; Verhaak, A. C. M.; Coenen, J. W. E. Gas Phase Benzene Hydrogenation on a Nickel Silica Catalyst. II. Gravimetric Experiments of Benzene, Cyclohexene and Cyclohexane Adsorption and Benzene Hydrogenation. *J. Catal.* **1976**, *44*, 217.

(14) Franco, H. A.; Philips, M. J. Gas Phase Hydrogenation of Benzene on Supported Nickel Catalysts. *J. Catal.* **1980**, *63*, 346.

(15) Martin, G. A.; Dalmon, J. A. Benzene Hydrogenation over Nickel Catalysts at Low and High-Temperatures−Structure-Sensitivity and Copper Alloying Effects. *J. Catal.* **1982**, *75*, 233.

(16) Keane, M. A.; Patterson, P. M. Compensation Behaviour in the Hydrogenation of Benzene, Toluene and *o*-Xylene over Ni/SiO_2−Determination of True Activation Energies. *J. Chem. Soc., Faraday Trans.* **1996**, *92*, 1413.

(17) Marécot, P.; Paraiso, E.; Dumas, J. M.; Barbier, J. Benzene Hydrogenation on Nickel Catalysts−Role of Weakly Bound Hydrogen. *Appl. Catal.* **1991**, *74*, 261.

(18) Suzuki, M.; Tsutsumi, K.; Takahashi, H. Characterization and Catalytic Activity of Nickel-Zeolite Catalysts. 1. Reduction Properties of Nickel Ions in Zeolites. *Zeolites* **1982**, *2*, 51.

(19) Coughlan, B.; Keane, M. A. The Hydrogenation of Benzene over Nickel-Supported Y-Zeolites. 1. A Kinetic Approach. *Zeolites* **1991**, *11*, 12.

(20) Coughlan, B.; Keane, M. A., The Hydrogenation of Benzene over Nickel-Supported Y-Zeolites. 2. A Mechanistic Approach. *Zeolites* **1991**, *11*, 483.

(21) van Meerten, R. Z. C.; Coenen, J. W. E. Gas Phase Benzene Hydrogenation on a Nickel−Silica Catalyst. IV. Rate Equations and Curve Fitting. *J. Catal.* **1977**, *46*, 13.

(22) van Meerten, R. Z. C.; Morales, A.; Barbier, J.; Maurel, R. Isotopic Effects in the Hydrogenation and Exchange of Benzene on Platinum and Nickel. *J. Catal.* **1979**, *58*, 43.

(23) Bond, G. C.; Cunningham, R. H.; Slaa, J. C. What do we Mean by Catalytic Activity. *Top. Catal.* **1994**, *1*, 19.

(24) Völter, J. A π-Complex Mechanism for Catalytic Hydrogenation of the Benzene Ring. *J. Catal.* **1964**, *3*, 297.

(25) Rahaman, M. V.; Vannice, M. A. The Hydrogenation of Toluene and Ortho-Xylene, Meta-Xylene and Para-Xylene over Palladium. 1. Kinetic Behaviour and Ortho-Xylene Isomerization *J. Catal.* **1991**, *127*, 251.

(26) Lindfors, L. P.; Salmi, T.; Smeds, S., Kinetics of Toluene Hydrogenation on Ni/Al_2O_3 Catalyst. *Chem. Eng. Sci.* **1993**, *22*, 3813.

(27) Lindfors, L. P.; Salmi, T. Kinetics of Toluene Hydrogenation on a Supported Ni Catalyst. *Ind. Eng. Chem. Res.* **1993**, *32*, 34.

(28) Smeds, S.; Murzin, D.; Salmi, T. Kinetics of *m*-Xylene Hydrogenation on Ni/Al_2O_3. *Appl. Catal. A* **1996**, *141*, 207.

(29) Smeds, S.; Murzin, D.; Salmi, T. Gas-Phase Hydrogenation of *o*-Xylene and *p*-Xylene on Ni/Al_2O_3. *Appl. Catal A* **1996**, *145*, 253.

(30) Smeds, S.; Salmi, T.; Murzin, D., Gas-Phase Hydrogenation of o- and *p*-Xylene on Ni/Al_2O_3, *Appl. Catal A*: *General* **1997**, *150*, 115.

(31) Keane, M. A., The Hydrogenation of o-, m- and *p*-Xylene over Ni/SiO_2, *J. Catal.* **1997**, *166*, 347.

(32) Bond, G. C.; Hooper, A. D.; Slaa, J. C.; Taylor, A. O. Kinetics of Metal-Catalysed Reactions of Alkanes and the Compensation Effect. *J. Catal.* **1996**, *163*, 319.

(33) Keane, M. A. The Role of Catalyst Activation in the Enantioselective Hydrogenation of Methyl Acetoacetate over Silica-Supported Nickel-Catalysts. *Can. J. Chem.* **1994**, *72*, 372.

(34) Ruthven, D. M. A Simple Method of Calculating Mass Transfer Effects for Heterogeneous Catalytic Gas Reactions. *Chem. Eng. Sci.* **1968**, *23*, 759.

(35) Mears, D. E. Tests for Transport Limitations in Experimental Catalytic Reactors. *Ind. Eng. Chem. Process Des. Dev.* **1971**, *10*, 541.

(36) Coughlan, B.; Keane, M. A. Adsorption of Benzene on a Range of Activated Y-Zeolites. *J. Chem. Soc., Faraday Trans.* **1990**, *86*, 3961.

(37) Stull, D. R.; Westrum, E. F., Jr.; Sinke, G. C. *The Chemical Thermodynamics of Organic Compounds*; John Wiley: New York, 1969.

(38) Butt, J. B. *Reaction Kinetics and Reactor Design*; Prentice Hall: Englewood Cliffs, NJ, 1980.

(39) Tétényi, P. Hydrogenation of Aromatic-Hydrocarbons over Supported Pt Catalysts−Comment. *J. Catal.* **1994**, *147*, 601.

(40) Konyukhov, V. Yu.; Tret'yakov, S. D.; Zykskin, A. G.; Kul'kova, N. V.; Temkin, M. I. Kinetics of Liquid Phase Hydrogenation of Benzene on Palladium Catalysts and Hydrogenation of Toluene on Palladium and Platinum Catalysts. *Kinet. Catal.* **1987**, *28*, 317.

(41) Lin, S. D.; Vannice, M. A. Hydrogenation of Aromatic-Hydrocarbons over Supported Pt Catalysts. 2. Toluene Hydrogenation. *J. Catal.* **1993**, *143*, 554.

(42) Patterson, W. R.; Rooney, J. J. An Explanation of the Compensation Effect in Catalysis. *J. Catal.* **1994**, *146*, 310.

(43) Martin, G. A. Variation of the Number of Metal Atoms Involved in Active-Sites and of the True Activation-Energy of Hydrocarbon Conversion and CO Hydrogenation over Metals. *Bull. Soc. Chim. Belg.* **1996**, *105*, 131.

(44) Galwey, A. K. Compensation Effect in Heterogeneous Catalysis. *Adv. Catal.* **1977**, *26*, 247.

(45) Pope, C. G. Sorption of Benzene, Toluene and Para-Xylene on Silicalite and H-ZSM5. *J. Phys. Chem.* **1986**, *90*, 835.

(46) Babernics, L.; Tétényi, P. Investigation of Benzene Adsorption on Cobalt Catalysts. *J. Catal.* **1970**, *17*, 35.

(47) Yung-Fang, Yu.; Chessick, J. J.; Zettlemoyer, A. C. Adsorption Studies on Metals. VIII. Monofunctional Organic Molecules on Reduced and Oxide-Coated Nickel and Copper. *J. Phys. Chem.* **1959**, *63*, 1626.

(48) Bellat, J.-P.; Simonot Grange, M. H. Adsorption of Gaseous *p*-Xylene and *m*-Xylene on NaY, KY and BaY Zeolites. 2. Modelling−Enthalpies and Entropies of Adsorption. *Zeolites* **1995**, *15*, 219.

(49) Chou, P.; Vannice, M. A. Benzene Hydrogenation over Supported and Unsupported Palladium. 2. Reaction Model. *J. Catal.* **1987**, *107*, 140.

(50) Lin, S.-D.; Vannice, M. A. Toluene Hydrogenation over Supported Platinum Catalysts. In *Proceedings of the 10th International Congress on Catalysis*; Guczi, L., Solymosi, F., Tétényi, P., Eds.; Elsevier: Amsterdam, 1993; p 861.

(51) Dean, J. A. *Handbook of Organic Chemistry*; McGraw-Hill: New York, 1987.

(52) Weder, G. *Chemisorption*: *An Experimental Approach*; Butterworth: London, 1976.

(53) Prinsloo, J. J.; Gravelle, P. C. Volumetric and Calorimetric Study of the Adsorption of Hydrogen at 296 K on Silica-Supported Nickel and Nickel−Copper Catalysts. *J. Chem. Soc., Faraday Trans. 1* **1980**, *76*, 2221.

(54) Smeds, S.; Salmi, T.; Lindfors, L. P.; Krause, O. Chemisorption and TPD Studies of Hydrogen on Ni/Al_2O_3. *Appl. Catal. A* **1996**, *144*, 177.

(55) Antonucci, P.; Vantruong, N.; Giordano, N.; Maggiore, R. Hydrogen Spillover Effects in the Hydrogenation of Benzene over Pt/Gamma Al_2O_3 Catalysts. *J. Catal.* **1982**, *75*, 140.

(56) Nagao, M.; Suda, Y. Adsorption of Benzene, Toluene and Chlorobenzene on Titanium Dioxide. *Langmuir* **1989**, *5*, 42.

(57) Laidler, K. J. *Chemical Kinetics*; Harper & Row: New York, 1987.

Received for review August 13, 1998
Revised manuscript received December 3, 1998
Accepted December 28, 1998

IE980540T